Numerical Solution of the Multidimensional Freezing Problem During Cryosurgery

Y. Rabin[1]
Department of Human Oncology,
Allegheny University of
the Health Sciences,
Pittsburgh, PA 15212-4772

A. Shitzer
Department of Mechanical Engineering,
Technion—Israel Institute of Technology,
Haifa 32000 Israel

A multidimensional, finite difference numerical scheme for the freezing process of biological tissues during cryosurgery is presented, which is a modification of an earlier numerical solution for inanimate materials. The tissues are treated as nonideal materials, freezing over a temperature range and possessing temperature-dependent thermophysical properties, blood perfusion, and metabolic heat generation. The numerical scheme is based on the application of an effective specific heat, substituting the intrinsic property, to include the latent heat effect within the phase transition temperature range. Results of the numerical solution were verified against an existing exact solution of a one-dimensional inverse Stefan problem in Cartesian coordinates. Results were further validated against experimental data available from the literature. The utility of the numerical solution for the design and application of cryodevices is demonstrated by parametric studies of the freezing processes around spherical and cylindrical cryoprobes. The parameters studied are the cryoprobe cooling power and the dimensions of the frozen region. Results are calculated for typical thermophysical properties of soft biological tissues, for angioma and for water.

Introduction

Heat transfer involving phase change in biological tissues is of great importance in medical applications. Examples are in the destruction of undesired tissues by freezing, termed cryosurgery (Oh, 1981; Orpwood, 1981; Onik et al., 1991), or in the preservation of desired tissues, referred to as cryopreservation (Akhtar et al., 1979; Fahy, 1981; Rubinsky, 1986). For the general solution for these problems, the biological tissues have to be considered as nonideal materials wherein thermophysical properties are temperature-dependent and phase transition occurs over a temperature range. Freezing problems in biological tissues must also include the thermal effects of blood perfusion and metabolic heat generation in the unfrozen regions.

There exist a limited number of analytical solutions for phase-change problems, all of which are one dimensional. Most of these solutions apply to simplified and idealized systems and are usually presented for inanimate materials (Carslaw and Jaeger, 1959; Lunardini, 1981). Exact solutions for freezing problems in biological tissues are presented for inverse problems only, of which boundary conditions are specified at the moving front (Rubinsky and Shitzer, 1976; Rabin and Shitzer, 1995). The complexity of multidimensional freezing problems suggests the application of numerical techniques. There seem to be two basic approaches for obtaining numerical solutions for these problems: One is based on a moving interface tracing technique (Shamsundar and Sparrow, 1975; Viskanta, 1983; Yoo and Rubinsky, 1986; Rabin, 1995) while the other is based on the enthalpy formulation (Lazaridis, 1970; Shamsundar and Sparrow, 1975; Hsiao and Chung, 1984).

The objectives of this paper are: (*a*) To present an explicit numerical solution for the multidimensional freezing problem, with application to cryosurgical processes in peripheral biological tissues. The solution is a modification of an earlier one developed for inanimate materials (Rabin and Korin, 1993) and includes the thermal effects of both blood perfusion and metabolic heat generation. (*b*) To demonstrate the utility of the numerical solution for design purposes, which will be done by showing that commonly used cryosurgical devices are not optimally designed.

Mathematical Formulation

It is customary to assume that heat transfer in biological tissues, characterized by a dense capillary network and low blood perfusion, can be modeled by the classical bioheat equation (Pennes, 1948):

$$C\frac{\partial T}{\partial t} = \nabla\cdot(k\nabla T) + \dot{w}_b C_b(T_b - T) + \dot{q}_{\text{met}} \qquad (1)$$

Although the general validity of this model is questionable, it was demonstrated recently that it can be used for engineering calculations and especially around a cryosurgical probe (Rabin et al., 1996a). The general boundary condition of Eq. (1) is given by:

$$-k\frac{\partial T}{\partial n} = U_s(T - T_\infty) \qquad (2)$$

The numerical solution of Eqs. (1) and (2) is developed for the following assumptions: (*a*) Phase transition occurs over a relatively wide temperature range, typically between −1°C (upper boundary) to −8°C (lower boundary), which is dependent on the tissue type (Altmann and Dittmer, 1971; Wessling and Blackshear, 1973). (*b*) No volume changes occur while the medium is undergoing phase transition. (*c*) The thermal conductivity is temperature and space dependent. (*d*) The volumetric specific heat is defined as an effective property incorporating the latent heat effect (Goodman, 1958; Voller, 1986). Based on experimental data, this effective property is represented by two linear functions, both starting at the intrinsic specific heat values at the phase transition temperature boundaries, and intersecting at a peak temperature of −3°C. The slopes of the linear functions are chosen such that the integral of this property over the phase transition temperature range equals the phase transition enthalpy changes (Bonacina et al., 1974; Comini and del

[1] Current address: Department of Mechanical Engineering, Technion, Haifa 32000, Israel. Email: yoed@tx.technion.ac.il.

Contributed by the Bioengineering Division for publication in the JOURNAL OF BIOMECHANICAL ENGINEERING. Manuscript received by the Bioengineering Division June 25, 1995; revised manuscript received February 12, 1997. Associate Technical Editor: J. J. McGrath.

Giudice, 1976). (*e*) Blood perfusion is temperature and space dependent and exists in the unfrozen region only. (*f*) The temperature of blood entering the tissue is uniform in space, a condition particularly applicable to peripheral tissues, characterized by a dense capillary network and relatively low blood perfusion. (*g*) Metabolic heat generation rate decreases exponentially with temperature in the unfrozen region (Eberhart, 1985).

Equation (1) is rewritten in a finite differences form for a typical numerical grid point i, j, k, for the three-dimensional case, independent of the coordinate system:

$$C_{i,j,k}\frac{T^{p+1}_{i,j,k}-T^{p}_{i,j,k}}{\Delta t}=\frac{1}{\Delta V_{i,j,k}}\sum_{l,m,n}\frac{T^{p}_{l,m,n}-T^{p}_{i,j,k}}{R_{l,m,n-i,j,k}}+(\dot{w}_bC_b)_{i,j,k}(T_b-T^{p+1}_{i,j,k})+(\dot{q}_{\mathrm{met}})_{i,j,k} \quad (3)$$

where l, m, and n are spatial indices for all the grid points in the neighborhood of node i, j, k. Contrary to common practice, the heat source term of blood perfusion in Eq. (3) is specified at time level $p + 1$, although the other terms on the right-hand side of the equation are written at time level p. This way of presentation is motivated by stability considerations, which are discussed hereafter. Rearrangement of Eq. (3) yields:

$$T^{p+1}_{i,j,k}=\frac{\Delta t}{\Delta V_{i,j,k}[C_{i,j,k}+(\dot{w}_bC_b)_{i,j,k}\Delta t]}\sum_{l,m,n}\frac{T^{p}_{l,m,n}-T^{p}_{i,j,k}}{R_{l,m,n-i,j,k}}+\frac{\Delta t[(\dot{w}_bC_b)_{i,j,k}T_b+(\dot{q}_{\mathrm{met}})_{i,j,k}]+C_{i,j,k}T^{p}_{i,j,k}}{C_{i,j,k}+(\dot{w}_bC_b)_{i,j,k}\Delta t} \quad (4)$$

where the thermophysical properties, the blood perfusion, and the metabolic heat generation are temperature dependent and thus have to be evaluated at each time level for each grid point.

The thermal resistance to heat transfer by conduction from grid point i, j, k to its neighboring grid points l, m, n is given by:

$$R_{l,m,n-i,j,k}=\left[\frac{\Delta\eta}{2kA}\right]_{l,m,n}+\left[\frac{\Delta\eta}{2kA}\right]_{i,j,k} \quad (5)$$

where η is substituted by x in the Cartesian geometry and by r in the cylindrical and spherical geometries. The heat transfer area by conduction, A, is expressed for the cylindrical geometry by:

$$A=\begin{cases}(r\pm\Delta r/4)\Delta\theta\Delta z & \eta=r\\ \Delta r\Delta z & \eta=\theta\\ r\Delta\theta\Delta r & \eta=z\end{cases} \quad (6)$$

For a one-dimensional heat conduction case in a spherical geometry, A is given by:

$$A=4\pi^2(r\pm\Delta r/4)^2 \quad (7)$$

The thermal resistance to heat transfer by convection from a boundary grid point i, j, k to the surroundings, at temperature T_s, is given by:

$$R_{s-i,j,k}=\frac{1}{A_{i,j,k}U_s} \quad (8)$$

where T_s replaces $T_{i,j,k}$ in Eq. (4).

Using standard stability analysis techniques (Carnahan et al., 1969), it can be shown that the stability criterion for the case of no blood perfusion is:

$$\Delta t\le\left[\frac{(\Delta VC)_{i,j,k}}{\sum_{l,m,n}(1/R_{l,m,n-i,j,k})}\right]_{\min} \quad (9)$$

It can further be shown that the stability of this numerical scheme increases with the inclusion of the blood perfusion term. This is due to the specific formulation of the blood perfusion term for time level $p + 1$. Rewriting this term at time level p would result in a decrease in stability as blood perfusion increases. For example, computer simulations were performed to indicate the stability limits for the general case of heat transfer in unfrozen tissues. A one-dimensional problem and typical thermophysical properties of soft tissues were chosen, and a step function was forced at the boundary, from an initial temperature of 37°C down to 0°C. Solving with the blood perfusion term written at time level p results in maximal time steps of 3.6, 12, 23, and 45 s, for space intervals of 1, 2, 3, and 5 mm, respectively. However, solving the same problems with the blood perfusion term written at time level $p + 1$, Eq. (3), results in increase of 6, 17, 39, and 100 percent, respectively, of the maximal time step for the cases described above.

The stability criterion presented above is necessary but not sufficient for calculating the maximal time step. An additional criterion is derived from energy conservation considerations. Time steps should be selected such that the temperature at each grid point of the phase transition region would change over a number of successive time steps. This will ensure that the latent heat effect is included in its entirety by the function representing the effective specific heat.

The stability criterion, Eq. (9), requires relatively short time intervals, which seems to be the major disadvantage of the proposed numerical scheme. For example, time steps in the range of 0.5 to 5 s are required for typical thermophysical properties of biological tissues, Table 1, and for space intervals of 1 mm in a three-dimensional problem. Therefore, it seems that any unconditionally stable numerical scheme would be preferable for the solution of the freezing problem, as there are no limitations on the length of time intervals. Regardless of the chosen numerical technique, the nature of the freezing process during cryosurgery, i.e., dramatic changes in thermophysical properties and steep temperature gradients, will demand a rela-

Nomenclature

A = area, m^2
C = volumetric specific heat, J/m^3 - °C
d = cryoprobe diameter, m
k = thermal conductivity, W/m-°C
L = length of the cylindrical cryoprobe active surface, m
n = unit normal coordinate, m
$\dot{q}$ = volumetric heat source, W/m^3
r, θ, z = cylindrical coordinates
R = thermal resistance to heat flow, °C/W
S_j = location of freezing front for cylindrical cryoprobe, Fig. 3, in radial ($j = 1$) and axial ($j = 2$) directions
t = time, s
T = temperature, °C
U = heat transfer coefficient, W/m^2-°C
V = volume, m^3
$\dot{w}$ = blood perfusion rate = $ml_b/ml_t - s$
η = general coordinate

Subscripts

b = blood
i, j, k = calculated grid point
l, m, n = neighbor grid point to the calculated one
met = metabolic
ml = upper boundary of phase transition
ms = lower boundary of phase transition
p = time level
s = boundary surface
t = tissue
∞ = infinity

Table 1 Typical thermophysical properties of water (Fletcher, 1970), soft biological tissues (Chato, 1985), and angioma (Comini and del Guidice, 1976)

	Water	Soft Biological Tissues	Angioma
Initial temperature	37°C	37°C	37°C
Upper limit of phase transition	0°C	-1°C	-1°C
Peak temperature of phase transition	-	-3°C	-3°C
Lower limit of phase transition	-	-8°C	-8°C
Blood temperature	-	37°C	37°C
Thermal conductivity of the unfrozen tissue, W/m-°C	0.6	0.5	0.56
Thermal conductivity of the frozen tissue, W/m-°C	2.25	2	2.22
Specific heat of the unfrozen tissue, MJ/m^3-°C	4.18	3.6	3.89
Specific heat of the frozen tissue, MJ/m^3-°C	1.13	1.8	2.01
Latent heat, MJ/m^3	331.7	250	250
Blood heat source, $\dot{w}_b C_b$, kW/m^3-°C	-	≤40	48.5
Metabolic heat generation, kW/m^3	-	33.8	33.8

tively fine numerical grid distribution. In turn, this will demand a relatively short time interval from energy conservation considerations, as mentioned above. For example, a one-dimensional modified Crank–Nicholson technique has been recently presented (Rabin and Shitzer, 1996), which is suitable for both inverse and ordinary phase-change problems. It is shown there that four to five numerical grid points are required within the phase transition temperature range, at any given time. The phase transition temperature range thickness was about 1 mm and, therefore, a relatively fine numerical grid was required. Although the Crank–Nicholson technique is unconditionally stable in nature, time intervals on the order of 1 s were required in order to satisfy the energy conservation criterion presented above. Therefore, the unconditionally stable numerical techniques do not automatically guarantee shorter time intervals for the particular problem of freezing of biological tissues. The application of implicit numerical schemes with approximately the same time intervals as required for the explicit numerical scheme suggested here will become more questionable for two-dimensional and three-dimensional freezing problems.

Finally, the explicit nature of the proposed numerical scheme demands a relatively small computer memory, which enables large-scale computer simulations, e.g., for the optimization of multiprobe cryosurgical operations. A comparison of typical matrix sizes required for a typical finite elements numerical scheme and a numerical solution similar to the one suggested here is presented by Rabin and Korin (1993).

Results and Discussion

The former version of the numerical solution, not including the thermal effects of blood perfusion and metabolic heat generation (Rabin and Korin, 1993), was validated against two exact solutions of the ordinary Stefan problem (Carslaw and Jaeger, 1959). It was also validated against two-dimensional solutions involving mixed boundary conditions (Lazaridis, 1970; Hsiao and Chang, 1984). Therefore, examination of the present numerical solution is focused on the blood perfusion term. This is done by comparing its predictions with those of an exact solution of the one-dimensional problem (Rabin and Shitzer, 1995). Results showed very good conformity of the two solutions.

The required cooling power and the propagation of the freezing front are studied next, for a one-dimensional case with spherical geometry. Radial heat flow in a spherical geometry is assumed to simulate a superficial cryotreatment. The actual cooling power of a cryoprobe is determined by both its internal structure and by the surrounding tissue, from which heat is absorbed. The lower bound design value for this quantity may be estimated by assuming that the internal structure of the cryoprobe is made of highly conductive materials, and thus the dominant resistance to heat flow resides in the surrounding tissue.

Two cases were considered in which the cooling effects are produced by either the expansion of a high pressure gas (Joule-Thomson effect) or by boiling. The lowest temperatures achievable for these cases were assumed at −120°C (argon or nitrogen gas) and −196°C (liquid nitrogen), respectively. The temperature forcing functions at the surface of the cryoprobe were constructed of two linear segments. The first segment began at a normal tissue temperature of 37°C and dropped to the lowest temperature in 60 s, producing cooling rates of about 160°C/min and 230°C/min at the surface of the cryoprobe, respectively. In the second segment the temperature remained constant, at this low level, throughout the duration of the application. These cooling protocols can be expected from high performance cryoprobes, especially in superficial cryotreatments where only a part of the cryoprobe is in direct contact with the tissue, and where the cryoprobe feeding tube can be relatively large. Each case was additionally examined for two conditions: (*a*) no blood perfusion, and (*b*) a specific blood heat source value of $\dot{w}_b C_b = 10\ kW/m^3$-°C. Thermophysical properties of the biological tissue are presented in Table 1. The range of spherical cryoprobe diameters considered are 5, 15, and 25 mm with the latter representing an upper bound for engineering design.

Figure 1 shows the locations of the two interfaces bounding the phase transition range, designated by T_{ml} and T_{ms}, for the three different spherical cryoprobes. As is to be expected for this geometry, the interface velocities decrease as the radii of the ice balls increase. The gaps between the interfaces widen continuously, indicating the thickening of the phase transition region. The effect of blood perfusion on the interface location is shown to slow down the freezing front propagation for the same operating parameters, as is to be expected.

Figure 2 shows the cooling power of the cryoprobe. Values were calculated by multiplying the temperature gradient adjacent to the cryoprobe surface by the thermal conductivity of the frozen region and the surface area of the cryoprobe. The actual cooling power in a specific application is calculated by

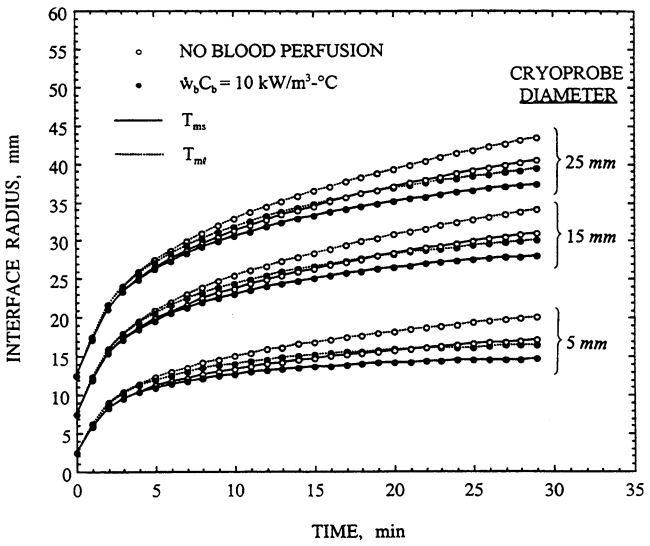

Fig. 1 Freezing front propagation around spherical cryoprobes in soft biological tissues, for zero and 10 kW/m^3 − °C heat sources due to blood perfusion. T_{ms} = −8°C and T_{ml} = −1°C represent the lower and upper boundaries of phase transition.

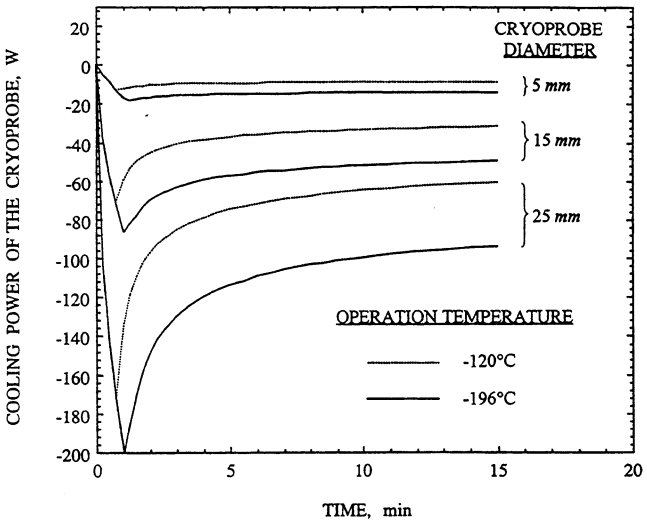

Fig. 2 Cooling power absorbed by spherical cryoprobes for two operating temperatures and a heat source due to blood perfusion of 10 kW/m^3 – °C

multiplying the values presented in Fig. 2 by the relative portion of the active surface of the cryoprobe that is in contact with the cryotreated tissue. As seen in Fig. 1, the differences in the freezing front locations between the cases of no blood perfusion and blood perfusion are not large. It follows that similar temperature distributions can be expected to develop in the frozen region of these two cases and, therefore, small differences in the cooling powers are to be expected. Thus, Fig. 2 presents results for the case of blood perfusion only. As can be expected, the cooling power required to initiate the process (first stage) is much higher than that required after the cryoprobe had reached its constant lowest temperature. From this figure it may be deduced that the cooling power of the cryoprobe tends to approach a constant value in time asymptotically. The power required for the case where the lowest cryoprobe temperature is −120°C (Joule-Thomson effect), is about 35 to 40 percent lower than that required for the case of −196°C cryoprobe temperature (liquid nitrogen).

A parametric study of a two-dimensional and axisymmetric cylindrical cryoprobe is addressed next, as is presented schematically in Fig. 3. The parameters under study are the same as for the spherical geometry, i.e., the cryoprobe cooling power and the frozen region dimensions. This study includes three freezing media: water, a medium having typical thermophysical properties of soft biological tissues, and an angioma. The thermophysical properties are listed in Table 1. Although phase transition of pure water occurs at a single temperature, it is assumed to freeze over the same temperature range typical of biological tissues for the purposes of the present parametric study. Extremely high blood perfusion is assumed in this study, of 40 and 48.5 kW/m^3 – °C for internal soft body tissues and for an angioma, respectively. The freezing front in this study is defined by the lower boundary of the phase transition temperature range, i.e., −8°C, which indicates the boundary enclosing the completely frozen region.

This study includes a wide range of cryoprobe dimensions considered suitable for minimal-invasive cryosurgery. The diameters under consideration vary between 2 mm, which may be considered as very fine for a minimal-invasive procedure, and up to 7 mm. The length of the cryoprobe active surface, L (Fig. 3), varies between 5 and 30 mm.

The cooling protocol considered here includes a constant cooling rate of 100°C/min at the cryoprobe surface, from a normal body temperature of 37°C down to −196°C, which remain constant thereafter. An average cooling rate of 100°C/min

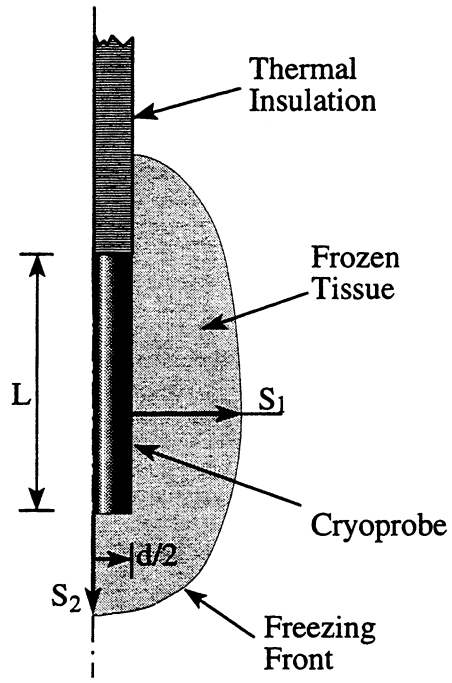

Fig. 3 Schematic presentation of an axi-symmetric freezing problem around a cylindrical cryoprobe used for a parametric study of minimal-invasive cryosurgery

is deemed reasonable for a low cooling power cryoprobe in an uncontrolled cryoprotocol. The process is terminated after 10 minutes, as the cooling power absorbed from the tissue reaches almost its steady-state condition. It is noted that the time required to reach steady state is a weak function of the cryoprobe dimensions; smaller cryoprobes will reach steady state faster, e.g., Fig. 2. A cryoprotocol duration of 10 minutes at −196°C was chosen for all cases to compare the performance of the cryoprobes. Two time points are defined for the analysis: *A*—when the cryoprobe temperature reaches −196°C for the first time, and *B*—when the heat transfer process approaches a steady-state condition (assumed after 10 minutes in this study).

The computed cryoprobe cooling powers are listed in Table 2. The cooling power was calculated by integrating the products of the thermal conductivity and the temperature gradient over

Table 2 Calculated cooling powers absorbed by cylindrical cryoprobes, W

d	Freezing	L = 5 mm		L = 10 mm		L = 20 mm		L = 30 mm	
mm	Medium	A	B	A	B	A	B	A	B
2	water	12.1	11.5	18.6	17.0	31.3	26.7	43.7	36.0
	tissue	9.1	8.1	14.8	12.7	26.2	21.3	37.5	29.6
	angioma	9.9	8.9	16.3	14.1	28.7	23.5	41.0	32.6
3	water	15.0	14.8	23.6	21.2	38.7	32.5	53.5	43.2
	tissue	11.5	10.1	18.4	15.5	32.1	25.5	45.6	35.1
	angioma	12.6	11.1	20.2	17.2	35.1	28.1	49.9	38.6
5	water	23.5	21.6	32.1	27.8	51.2	42.6	70.1	55.0
	tissue	16.2	13.8	25.1	20.5	42.7	32.7	60.0	44.4
	angioma	17.7	15.2	27.5	22.6	46.5	36.0	65.1	48.8
7	water	28.2	26.9	40.3	35.8	63.0	51.9	85.5	66.3
	tissue	20.7	17.2	31.4	25.0	52.3	39.1	72.8	52.5
	angioma	22.7	20.0	34.4	27.6	56.8	43.0	79.1	57.7

A - time at which cryoprobe temperature reaches -196°C

B - 10 min afterwards (approaching a steady state)

the cryoprobe active surface for the listed time. As expected and qualitatively similar to the spherical case, the cooling power near a steady-state condition (at time point B) is significantly lower than that required during the first stage of cooling (which ends at time point A). This difference increases as the length and diameter of the cryoprobe are increased. The calculated cooling power near a steady-state condition can be used as an engineering design parameter, regardless of the particular cooling protocol applied. In the range of the values presented, this difference ranges between 5 percent for the smallest cryoprobe in water to 37 percent for the largest cryoprobe in an angioma.

It can further be seen from Table 2 that the cooling power required for freezing of an angioma is higher than that required for the case of typical soft biological tissues, primarily due to the higher blood perfusion. However, water freezing requires a higher cooling power than is required for freezing of biological tissues, a difference that increases with the cryoprobe diameter and decreases with its length. This can be explained as follows. On the one hand, biological tissues have blood perfusion and metabolic heat sources, which tend to increase the required cryoprobe cooling power. One the other hand, the latent heat of water is higher, a property that tends to result in a decrease of the frozen region size and thus tends to increase the temperature gradients within the frozen region and, in turn, to increase the required cooling power. The balance between these two factors determines the differences in cooling powers. The minimal difference, in the range of the present parametric study, is 22 percent and is obtained for the case of $d = 2$ mm and $L = 30$ mm, a configuration that can almost be considered as an infinite cylinder from heat transfer considerations. The maximal difference is 56.5 percent and is obtained for the case of $d = 5$ mm and $L = 5$ mm, which can be approximated as a spherical cryoprobe.

The dimensions of the frozen region are addressed next. Tables 3 and 4 present the freezing front locations in the radial and axial directions, S_1 and S_2, respectively. In general, only minor differences are observed in the interface location in the S_1 direction, of about 5 percent for each cryoprobe configuration. Significant differences are found in the S_2 direction, where the freezing front of water propagates much slower due to the latent heat effect as discussed above. It can be seen that for freezing of an angioma, the freezing front propagates a bit faster and farther than for the case of typical soft biological tissues. This can be explained by the fact that both thermal conductivities, of the unfrozen and of frozen regions, are higher for the angioma, Table 1. Tables 3 and 4 can be used to select the appropriate cryoprobe dimensions for a desired frozen region size.

Table 3 Calculated freezing front locations around cylindrical cryoprobes in radial S_1 direction (Fig. 3), mm

d mm	Freezing Medium	L = 5 mm		L = 10 mm		L = 20 mm		L = 30 mm	
		A	B	A	B	A	B	A	B
2	water	5.8	8.7	6.7	11.1	7.4	13.8	7.4	15.0
	tissue	5.8	9.2	6.9	11.2	7.3	13.5	7.4	14.5
	angioma	6.2	9.3	7.0	11.5	7.6	13.9	7.6	14.9
3	water	6.6	9.7	7.6	12.3	8.2	15.1	8.4	16.4
	tissue	6.9	10.5	7.7	12.5	8.2	14.8	8.3	15.9
	angioma	7.1	10.6	7.9	12.8	8.5	15.3	8.6	16.4
5	water	7.9	11.6	9.0	14.3	9.7	17.2	10.2	18.5
	tissue	8.3	12.6	9.2	14.7	9.7	17.0	10.0	18.2
	angioma	8.5	12.8	9.4	15.0	10.1	17.5	10.2	18.5
7	water	9.2	13.2	10.3	16.1	11.2	19.0	11.3	20.9
	tissue	9.6	14.5	10.5	16.5	11.2	18.8	11.2	20.0
	angioma	9.8	14.6	10.7	16.8	11.3	19.3	11.3	20.8

A - time at which cryoprobe temperature reaches -196°C

B - 10 min afterwards (approaching a steady state)

Table 4 Calculated freezing front locations around cylindrical cryoprobes in the axial S_2 direction (Fig. 3), mm

d mm	Freezing Medium	L = 5 mm		L = 10 mm		L = 20 mm		L = 30 mm	
		A	B	A	B	A	B	A	B
2	water	2.9	4.1	2.9	4.4	2.9	4.8	2.9	4.9
	tissue	4.1	7.4	4.3	7.9	4.3	8.3	4.3	8.4
	angioma	4.4	7.5	4.4	8.2	4.4	8.5	4.4	8.5
3	water	3.8	5.6	3.8	6.1	3.8	6.3	3.8	6.3
	tissue	5.1	8.6	5.1	9.3	5.1	9.5	5.1	9.5
	angioma	5.2	8.8	5.2	9.5	5.2	9.7	5.2	9.7
5	water	5.1	7.8	5.1	8.2	5.1	8.4	5.1	8.4
	tissue	6.1	10.6	6.1	11.2	6.1	11.5	6.1	11.5
	angioma	6.2	10.9	6.3	11.5	6.3	11.7	6.3	11.7
7	water	6.1	9.7	6.1	10.0	6.1	10.2	6.1	10.2
	tissue	6.9	12.3	7.0	12.7	7.0	13.0	7.0	13.0
	angioma	7.1	12.5	7.1	13.0	7.1	13.4	7.1	13.5

A - time at which cryoprobe temperature reaches -196°C

B - 10 min afterwards (approaching a steady state)

In order to provide the reader with some insight, the diameter of the calculated frozen region has been compared with available experimental data from the literature. A 3.4-mm-dia cylindrical cryoprobe of AccuProbe (CryoMedical Sciences, Inc.; Chang et al., 1994) has been chosen for that comparison, which has a 40-mm active surface length. The experiment has been performed in a 1.5 percent gelatin solution, which is assumed to have similar thermophysical properties to those of water. An average cooling rate of 100°C/min was assumed, based on the coolant temperature that returns from the cryoprobe, and an active surface temperature of −165°C has been reported. Figure 4 presents the comparison of the freezing front location and the cooling power required for this procedure as was calculated by the numerical solution.

The required cooling power, Table 2 and Fig. 4, indicates the minimal coolant flow rate required through the cryoprobe and, thus, determines the minimal performance desired from the coolant supply system for each cryoprobe. For the purposes of this discussion, the thermal efficiency of a cryosurgical de-

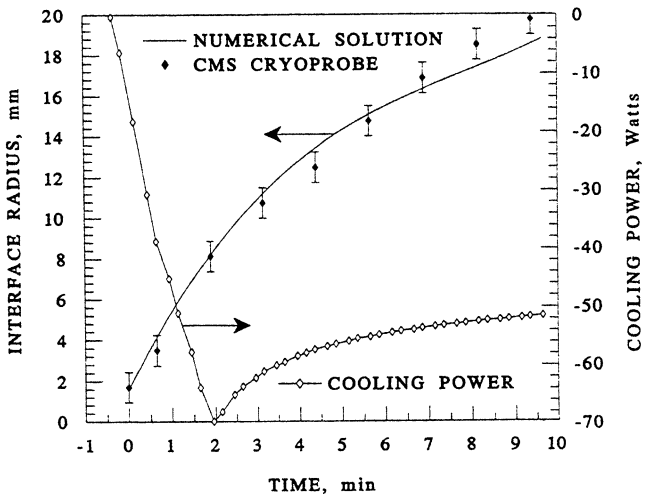

Fig. 4 Comparison of the freezing front location around a 3.4-mm cylindrical cryoprobe of AccuProbe system, as was measured experimentally (Chang et al., 1994) and as is predicted using the numerical scheme. The required cryoprobe cooling power was calculated by the numerical simulation.

vice is defined as the ratio of the actual energy absorbed from the cryotreated tissue to the maximal possible energy that the cryoprobe can absorb. Assuming maximal thermal efficiency at the cryoprobe, and assuming that most of the heat sink in a boiling effect-based cryoprobe is due to the coolant boiling, the minimal coolant flow rate can be calculated by dividing the required cooling power by the latent heat of the coolant. For example, a cryoprobe having a diameter of 3.4 mm and a length of 40 mm (AccuProbe, Fig. 4) requires a maximal cooling power of 70 W and an instantaneous cooling power of 51.5 W after 10 min of operation, Fig. 4. Taking into consideration the volumetric latent heat of liquid nitrogen (199 MJ/m^3), the minimal flow rates desired are 21.1 and 15.5 cm^3/min, respectively. Current liquid-nitrogen-based cryodevices are characterized by low thermal efficiency, which demands much higher coolant consumption and which, in turn, requires large and cumbersome coolant supply systems, such as that of CryoMedical Sciences, Inc. (Chang et al., 1994). The rate of coolant consumption of commercial cryodevices is generally not published; however, results presented in Table 2 indicate that compact cryodevices with much higher thermal efficiency can be designed. For example, a new cryodevice has been recently reported by Rabin et al. (1997), which was capable of freezing a water volume of 270 cm^3 within 13 min, using a triple-cryoprobe configuration, with a total liquid nitrogen consumption of 1050 cm^3. Assuming that most of the energy absorbed from the water is due to the latent heat of water freezing (331.7 MJ/m^3), the thermal efficiency of this cryodevice is 43 percent. This, among other things, serves to demonstrate the utility of the numerical solution in improving the design of more efficient cryosurgical systems.

Summary and Conclusions

A new multidimensional numerical solution applicable to freezing of biological tissues during cryosurgery is presented. The solution is a modification of an earlier one for inanimate materials and includes the effects of blood perfusion and metabolic heat generation. The new solution is explicit in nature and its stability criterion demands relatively short time intervals. However, it is argued that for typical conditions of cryosurgery, i.e., steep temperature gradients and strong variations of the thermophysical properties with temperature, an alternative implicit solution will not necessarily guarantee higher efficiency in the solution, especially in the three-dimensional case.

A very good agreement was found between the results of the new solution and an exact one of the inverse Stefan problem in biological tissues. A good agreement was further found between the numerical solution and experimental results available from the literature of a 3.4-mm cylindrical cryoprobe. Parametric studies of freezing around spherical and cylindrical cryoprobes are further presented, using typical parameters of a superficial and a minimal-invasive cryoprocedures, respectively. The results demonstrate the cooling power of the cryoprobes and typical dimensions of the frozen region for a range of operating parameters. Results indicate that common cryosurgical devices have a low thermal efficiency and a high coolant consumption.

Acknowledgments

This work was supported, in part, by the James H. Belfer Chair in Mechanical Engineering, by the Technion Vice President for Research Fund for the promotion of research, and by the Cancer Center, Allegheny University of the Health Sciences, Pittsburgh, PA.

References

Akhtar, T., Pegg, D. E., and Foreman, J., 1979, "The Effect of Cooling and Warming Rates on the Survival of Cryopreserved L-Cells," *Cryobiology,* Vol. 16, pp. 424–429.

Altman, P. L., and Dittmer, D. S., 1971, *Respiration and Circulation,* Federation of American Societies for Experimental Biology (Data Handbook), Bethesda, MD.

Bonacina, C., Comini, G., Fasano, A., and Primicerio, M., 1974, "On the Estimation of Thermophysical Properties in Nonlinear Heat Conduction Problems," *Int. J. Heat Mass Trans.,* Vol. 17, pp. 861–867.

Carnahan, B., Luther, H. A., and Wilkes, J. O., 1969, *Applied Numerical Methods,* Wiley, New York.

Carslaw, H. S., and Jaeger, J. C., 1959, *Conduction of Heat in Solids,* Clarendon Press, Oxford.

Chang, Z., Finkelstein, J. J., Ma, H., and Baust, J., 1994, "Development of a High-Performance Multiprobe Cryosurgerical Device," *Biomed. Inst. & Tech.,* Vol. 28, pp. 383–390.

Chato, J. C., 1985, "Selected Thermophysical Properties of Biological Materials," in: *Heat Transfer in Biology and Medicine,* Shitzer, A., and Eberhart, R. C., eds., Plenum Press, New York, pp. 413–418.

Comini, G., and del Giudice, S., 1976, "Thermal Aspects of Cryosurgery," ASME *Journal of Heat Transfer,* Vol. 98, pp. 543–549.

Eberhart, R. C., 1985, "Thermal Models of Single Organs," in: *Heat Transfer in Medicine and Biology,* A. Shitzer and R. C. Eberhart, eds., Plenum Press, New York, pp. 261–324.

Fahy, G. M., 1981, "Analysis of 'Solution Effect' Injury: Cooling Rate Dependence of the Functional and Morphological Sequelae of Freezing in Rabbit Renal Cortex Protected With Dimethy Sulfoxide," *Cryobiology,* Vol. 18, pp. 550–570.

Goodman, T. R., 1958, "The Heat Balance Integral and Its Application to Problems Involving a Change of Phase," *ASME Trans.,* Vol. 80, pp. 335–342.

Hsiao, J. H., and Chung, B. T. F., 1984, "An Efficient Algorithm for Finite Element Solution to Two-Dimensional Heat Transfer With Melting and Freezing," ASME Paper No. 84-HT-2.

Keanini, R. G., and Rubinsky, B., 1992, "Optimization of Multiprobe Cryosurgery," ASME *Journal of Heat Transfer,* Vol. 114, pp. 796–801.

Lazaridis, A., 1970, "A Numerical Solution for the Multidimensional Solidification (or Melting) Problem," *Int. J. Heat Mass Trans.,* Vol. 13, pp. 1459–1477.

Lunardini, V. L., 1982, *Heat Transfer in Cold Climates,* Van Nostrand, New York.

Oh, C., 1981, "One Thousand Cryohemorrhoidectomies: An Overview," *Dis. Colon Rectum,* Vol. 24, pp. 613–617.

Onik, G., Rubinsky, B., Zemel, R., Weaver, L., Diamond, D., Cobb, C., and Porterfield, B., 1991, "Ultrasound-Guided Hepatic Cryosurgery in the Treatment of Metastatic Colon Carcinoma," *Cancer,* Vol. 67 (4), pp. 901–907.

Orpwood, R. D., 1981, "Biophysical and Engineering Aspects of Cryosurgery," *Phys. Med. Biol.,* Vol. 26 (4), pp. 555–575.

Pennes, H. H., 1948, "Analysis of Tissue and Arterial Blood Temperature in Resting Human Forearm," *J. App. Phys.,* Vol. 1, pp. 93–122.

Rabin, Y., and Korin, E., 1993, "An Efficient Numerical Solution for the Multidimensional Solidification (or Melting) Problem Using a Microcomputer," *Int. J. Heat Mass Trans.,* Vol. 36, No. 3, pp. 673–683.

Rabin, Y., and Shitzer, A., 1995, "Exact Solution for the Inverse Stefan-Problem in Non-Ideal Biological Tissues," ASME *Journal of Heat Transfer,* Vol. 117, pp. 425–431.

Rabin, Y., 1995, "Approximate Solution of the Inverse-Stefan Problem in Cartesian, Cylindrical and Spherical Geometries," *Inverse Problems in Bioheat and Mass Transfer,* ASME HTD-Vol. 322/BED-Vol. 32, pp. 1–4.

Rabin, Y., Coleman, R., Mordohovich, D., Ber, R., and Shitzer, A., 1996a, "A New Cryosurgical Device for Controlled Freezing. Part II: In Vivo Experiments on Rabbits' Hindlimbs," *Cryobiology,* Vol. 33, pp. 93–105.

Rabin, Y., Julian, T. B., and Wolmark, N., 1997, "A Compact Cryosurgical Apparatus for Minimal-Invasive Cryosurgery," *Biomed. Inst. & Tech.,* Vol. 31, pp. 251–258.

Rabin, Y., and Shitzer, A., 1997, "Combined Solution of the Inverse Stefan Problem for Successive Freezing/Thawing in Nonideal Biological Tissues," ASME JOURNAL OF BIOMECHANICAL ENGINEERING, Vol. 119, pp. 146–152.

Rubinsky, B., 1986, "Recent Advances in Cryopreservation of Biological Organs and in Cryosurgery," *Proc. of IHTC,* pp. 307–316.

Rubinsky, B., and Shitzer, A., 1976, "Analysis of a Stefan-Like Problem in a Biological Tissue Around a Cryosurgical Probe," ASME *Journal of Heat Transfer,* Vol. 98, pp. 514–519.

Shamsundar, N., and Sparrow, E. M., 1975, "Analysis of Multidimensional Conduction Phase Change Problem Via the Enthalpy Model," ASME *Journal of Heat Transfer,* Vol. 97, No. 3, pp. 333–340.

Viskanta, R., 1983, "Phase Change Heat Transfer," *Solar Heat Storage: Latent Heat Material,* Lane, G. A., ed., CRC Press, FL.

Voller, V. R., 1986, "A Heat Balance Integral Based on the Enthalpy Formulation," *Int. J. Heat Mass Trans.,* Vol. 30, pp. 604–606.

Wessling, F. C., and Blackshear, P. L., 1973, "The Thermal Properties of Human Blood During Freezing Process," ASME *Journal of Heat Transfer,* Vol. 95, pp. 246–249.

Yoo, J., and Rubinsky, B., 1986, "A Finite Element Method for the Study of Solidification Processes in the Presence of Natural Convection," *Int. J. Numerical Methods Eng.,* Vol. 23, pp. 1785–1805.